

Greigite magnetosome membrane ultrastructure in '*Candidatus Magnetoglobus multicellularis*'

Fernanda Abreu,¹ Karen T. Silva,¹ Marcos Farina,²
Carolina N. Keim,¹ Ulysses Lins^{1*}

¹Professor Paulo de Góes Institute of Microbiology, Federal University of Rio de Janeiro, Rio de Janeiro, Brazil.

²Institute of Biomedical Sciences, School of Medicine, Federal University of Rio de Janeiro, Rio de Janeiro, Brazil

Received 23 December 2007 · Accepted 28 April 2008

Summary. The ultrastructure of the greigite magnetosome membrane in the multicellular magnetotactic bacteria '*Candidatus Magnetoglobus multicellularis*' was studied. Each cell contains 80 membrane-enclosed iron-sulfide magnetosomes. Cytochemistry methods showed that the magnetosomes are enveloped by a structure whose staining pattern and dimensions are similar to those of the cytoplasmic membrane, indicating that the magnetosome membrane likely originates from the cytoplasmic membrane. Freeze-fracture showed intramembrane particles in the vesicles surrounding each magnetosome. Observations of cell membrane invaginations, the trilaminar membrane structure of immature magnetosomes, and empty vesicles together suggested that greigite magnetosome formation begins by invagination of the cell membrane, as has been proposed for magnetite magnetosomes. [Int Microbiol 2008; 11(2):75-80]

Key words: '*Candidatus Magnetoglobus multicellularis*' · greigite · magnetotactic bacteria · magnetosome ultrastructure · cytochemistry

Introduction

Magnetotactic bacteria produce nano-scaled, membrane-enveloped magnetic-iron-containing crystals called magnetosomes as well as several other amorphous inclusions [20]. The mineral composition of the magnetosome can be either magnetite (Fe₃O₄) or greigite (Fe₃S₄) [7,12]. In unicellular magnetotactic bacteria, magnetosome chains are usually aligned with the axis of cellular movement, which imparts the cell with a magnetic moment that aligns the cell body along the local magnetic field while it swims propelled by flagella [33]. This results in net migration along magnetic field lines. Magnetite magnetosome biomineralization has mainly been investigated in cultivated species of the genus

Magnetospirillum, which produce cubo-octahedral, equidimensional crystals [33]; in those bacteria, the molecular mechanisms and cell biology of magnetosome formation are beginning to be elucidated. The data obtained from electron cryo-tomography of *Magnetospirillum magneticum* AMB-1 suggest that magnetosomes are permanent invaginations of the cell membrane rather than vesicles, as previously proposed [22]. This membrane contains numerous proteins involved in controlling magnetosome synthesis. In addition, the magnetosome membrane together with cytoskeleton elements is involved in aligning the magnetosomes as a chain [22,29,32].

Only a few strains of magnetotactic bacteria have been cultivated and all of them produce magnetite in magnetosomes. Nevertheless, the biomineralization of magnetite is considered to be controlled at the gene level because both the morphology and the size of the magnetite produced by magnetotactic bacteria are species-specific [7]. Bacterial magnetite typically has cube {100}, octahedron {111}, and dodecahedron {110} faces in crystals that are commonly elongated [10] or bullet-shaped [26–28,37]. In uncultured bacteria,

*Corresponding author: U. Lins

Instituto de Microbiologia Professor Paulo de Góes

Universidade Federal do Rio de Janeiro

21941-902, Rio de Janeiro, RJ, Brasil

Tel. +55-21225626738. Fax +55-2125608344

E-mail: ulins@micro.ufrj.br; ulysses.lins@gmail.com

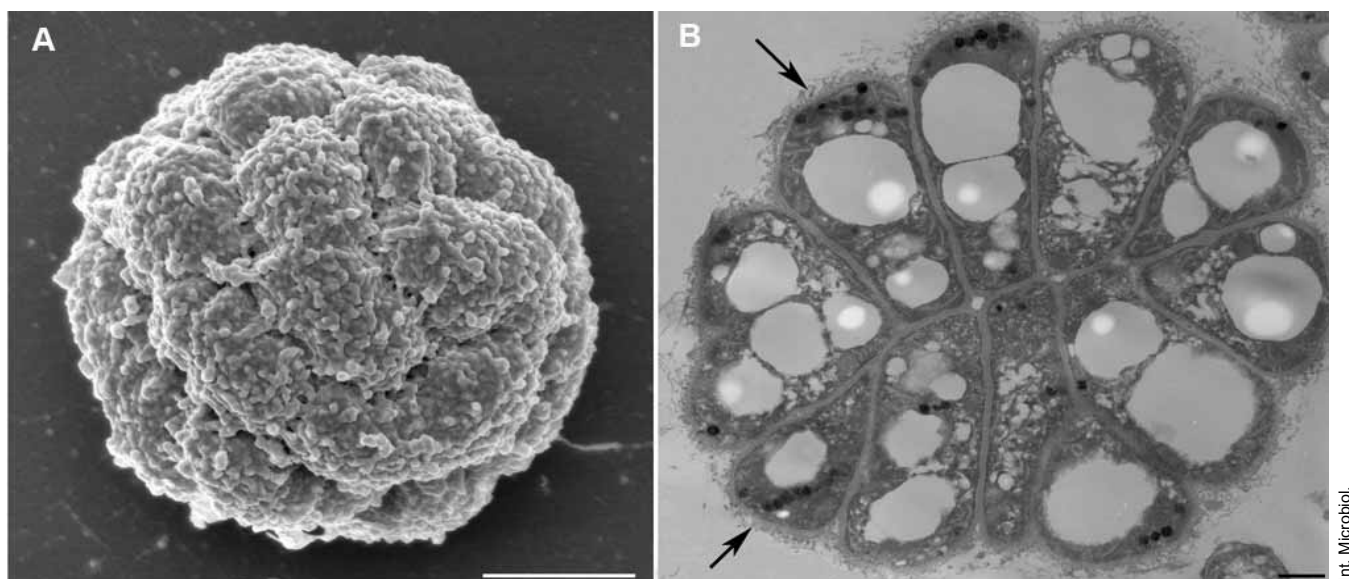


Fig. 1. (A) Scanning electron microscopy image of ‘*Candidatus Magnetoglobus multicellularis*’. (B) Transmission electron microscopy image of ‘*Candidatus Magnetoglobus multicellularis*’ showing magnetosomes (arrows). Scale bar = 1 μm in (A), and 300 nm in (B).

there are only a few reports on the nature of the membrane surrounding magnetite magnetosomes, possibly because of the difficulty in obtaining large numbers of cells for biochemical analysis [15]. Those studies proposed a protein matrix in *Magnetobacterium bavaricum* [15] and a magnetosomal organic matrix in unnamed rods and cocci [36].

‘*Candidatus Magnetoglobus multicellularis*’ [2] is the best characterized of the multicellular magnetotactic prokaryotes and the greigite-producing magnetotactic bacteria. Multicellular magnetotactic prokaryotes similar to ‘*Candidatus M. multicellularis*’ have been detected in the northern hemisphere [35]. Each individual consists of about 20 gram-negative bacterial cells, which are not viable when isolated [1]. The cells are organized side by side in a sphere (Fig. 1A) that swims in either straight or helical trajectories. Each cell contains iron sulfide magnetosomes (Fig. 1B) arranged in parallel chains [2,17,19,34]. Organization of the chains is necessary to impart an optimized net magnetic moment on the whole microorganism [38].

The lack of greigite-producing magnetotactic bacteria in pure culture has hampered efforts to study the biomineralization of greigite-containing magnetosomes. Most greigite magnetosomes occur in parallelepiped [8] or cuboctahedral shapes [30] with irregular borders. The modeled and measured size distribution of greigite crystals indicates that the growth of these crystals is not as strictly controlled as the growth of magnetite crystals in most magnetotactic species [4]. So far, it is unknown whether greigite magnetosome synthesis is membrane-regulated in the same way as reported for

magnetite magnetosomes [21,22,32]. In greigite-producing multicellular magnetotactic bacteria, a membrane has been identified [9,11,23,24], but neither its ultrastructure nor its composition has been unequivocally determined. In the present study, transmission electron microscopy (TEM) and cytochemical methods in which proteins and lipids are selectively stained were used to elucidate the ultrastructure of the magnetosome membrane of ‘*Candidatus Magnetoglobus multicellularis*.’

Materials and methods

Samples of water and sediment were collected at Araruama Lagoon (22°50' S, 42°13' W), Rio de Janeiro state, Brazil, and maintained in the laboratory for a few days. Samples of microorganisms were magnetically isolated using a specially designed glass flask and a home-made coil, as described [25]. Negative staining was done by dropping suspensions of microorganisms on formvar-coated copper grids, which were then washed with distilled water and stained for 1 min with a 2% phosphotungstic acid (PTA) solution.

For conventional TEM, the samples were fixed in 2.5% glutaraldehyde in 0.1 M cacodylate buffer prepared in lagoon water (pH 7.3), washed in the same buffer, post-fixed in 1% OsO_4 cacodylate buffer 0.1 M (pH 7.3) for 1 h in the dark, washed in the same buffer, dehydrated in an acetone series, and embedded in Polybed 812. For potassium-ferrocyanide cytochemistry, samples were fixed in 2.5% glutaraldehyde in 0.1 M cacodylate buffer prepared in lagoon water (pH 7.3) with 5 mM CaCl_2 for 2 h, washed in the same buffer, post-fixed in 1% OsO_4 cacodylate buffer 0.1 M (pH 7.3) with 5 mM CaCl_2 and 0.8% potassium ferrocyanide for 2 h in the dark, washed in 0.1 M cacodylate buffer (pH 7.3), dehydrated in an acetone series, and embedded in Polybed 812. For lipid contrast enhancement [3], samples were fixed in 2.5% glutaraldehyde in 0.1 M cacodylate buffer prepared in lagoon water (pH 7.3), washed in cacodylate buffer 0.1 M (pH 7.3), washed in imidazole

buffer 0.1 M (pH 7.5), post-fixed in an imidazole-buffered 1% OsO₄ solution, washed in the same buffer, dehydrated in an acetone series, and embedded in Polybed 812. Ultra-thin sections were obtained with a Reichert Ultracut ultramicrotome. All of the samples were stained with uranyl acetate and lead citrate except the imidazole cytochemistry grids, which were stained with lead citrate only. Ultra-thin sections were observed with a FEI Morgagni TEM at 80 kV or a JEOL 1200 FX TEM at 100 kV. Measurements were done in magnification-calibrated negatives with an AnalySIS 5.0 digital image analysis system.

For freeze-fracture experiments, samples were processed as described previously [17]. Briefly, the samples were fixed in 2.5% glutaraldehyde in 0.1 M cacodylate buffer prepared in lagoon water, washed in the same buffer, cryoprotected with 30% glycerol, and frozen by immersion in liquid Freon 22. The frozen samples were fractured in a Balzers freeze-fracture device and then sputtered with platinum at 45° and carbon at 90°. The replicas were cleaned with either 70% sodium hypochlorite or 70% sulfuric acid and observed in a Jeol 1200 EX TEM at 80 kV.

Results and Discussion

'*Candidatus Magnetoglobus multicellularis*' observed by light microscopy were very motile microorganisms that, because of their numerous magnetosome chains, responded promptly to an applied magnetic field. Each single cell of '*Candidatus Magnetoglobus multicellularis*' contained about 80 pleomorphic magnetosomes organized in 1–5 parallel chains within the cell. The magnetosomes were larger than those previously reported for other magnetotactic multicellular

Table 1. Statistical data on the magnetosomes of '*Candidatus Magnetoglobus multicellularis*' (n = 746)

	Mean	Minimum	Maximum	SD
Crystal length (nm)	88.3	57.3	178.8	11.5
Crystal width (nm)	65.5	24.4	124.1	9.8
Aspect ratio (width/length)	0.8	0.4	1.0	0.1

prokaryotes [4] (statistical data are summarized in Table 1). Ruptured cells released chains of magnetosomes that were enveloped by a thin coat of about 3.7 nm, which most probably corresponded to the magnetosome membrane (Fig. 2A). This membrane seemed to hold the magnetosomes together after their isolation (Fig. 2A), which suggested that the magnetosomes are either linked to each other or connected to a common structure, such as cytoskeleton filaments, as described for *Magnetospirillum magneticum* AMB-1 [22]. Post-fixation with imidazole-buffered OsO₄, a protocol known to stain lipids [3], evidenced an electron-dense membrane, 2.1-nm thick, around each magnetosome (Fig. 2B). Ultra-thin sections of samples that had not been stained with OsO₄ showed electron-dense layers of about 2.0 nm surrounding each magnetosome (Fig. 2C), whereas stained samples evidenced a thicker, electron-dense area of 6.1 nm (Fig. 2D).

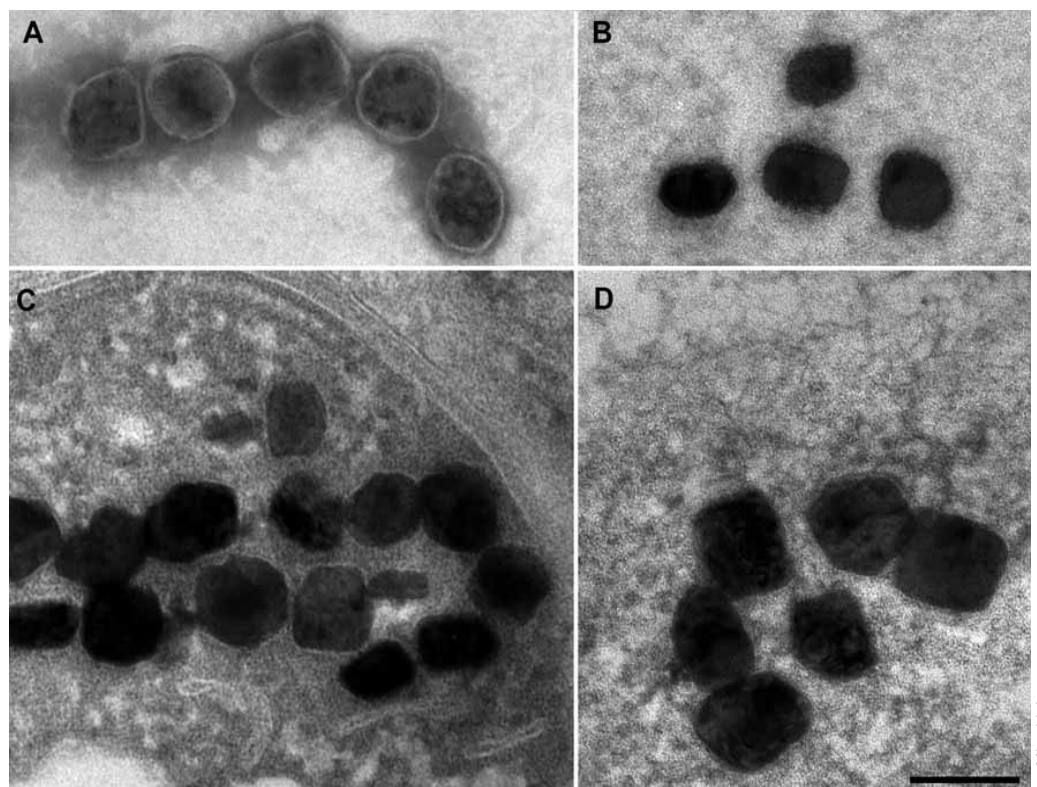


Fig. 2. Transmission electron microscopy images of '*Candidatus Magnetoglobus multicellularis*' magnetosomes. (A) Negative staining with 2% PTA shows the magnetosomes, with an electron-transparent layer surrounding each particle. (B) Imidazole cytochemistry shows an electron-dense region around the crystals. (C) Sample prepared without OsO₄ but stained with uranyl acetate and lead citrate. (D) Conventional processing using OsO₄. Note that the structure surrounding the magnetosome is clearly seen when OsO₄ is used, indicating the presence of unsaturated lipids typical of biological membrane. Scale bar = 100 nm.

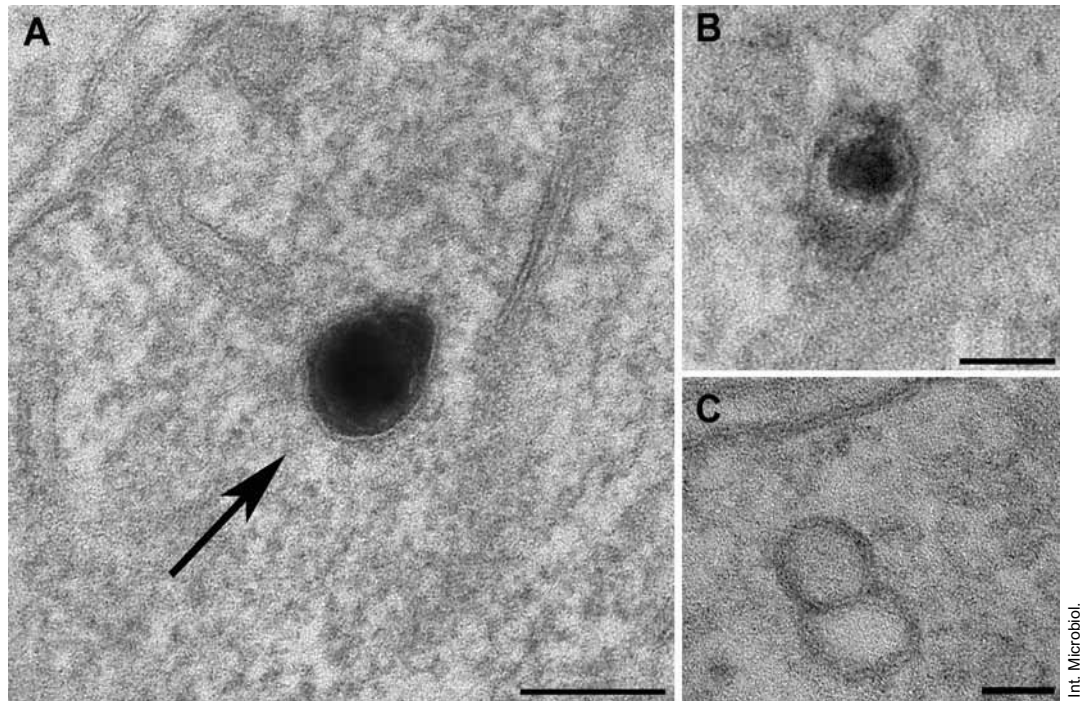


Fig. 3. Potassium ferrocyanide cytochemistry of the magnetosome membrane. (A) Detail of the border of a cell shows invaginations of the cell membrane (arrow) and a membrane similar to the cell membrane involving the magnetic crystal. The inner electron-dense layer of the magnetosome membrane is close to the crystal. (B) Immature magnetosome in the cytoplasm. (C) Empty vesicles presumably corresponding to empty, early magnetosomes. Scale bars = 100 nm in (A), and 50 nm in (B,C).

As seen in potassium-ferrocyanide cytochemical preparations, crystals present within the mature magnetosomes were enveloped by a 3.2-nm-thick structure (Fig. 3A). This electron-dense material coating the magnetosome crystals was similar in density and thickness to the cell membrane, which was 3.6-nm thick. In addition, the cytoplasm contained many vesicles invaginating from the cell membrane (Fig. 3A; arrow), as well as immature magnetosomes (Fig. 3B) and empty vesicles (Fig. 3C). The membrane of the empty vesicles was trilaminar in structure and 4-nm thick.

The variation in magnetosome membrane thickness in the different preparations was most likely due to differential osmium deposition or to enhancement by Ca^{2+} ions in the osmium-ferricyanide staining solution, as calcium is known to improve contrast in stained prokaryote membranes, and to post-staining with uranyl acetate and lead. Particularly in the ferricyanide or ferrocyanide methods, osmium deposition can be very irregular, with osmium penetrating well in some regions but not in others [16].

In freeze-fracture replicas, structures corresponding to the P-faces of vesicles about the same size as the magnetosomes were observed in the cytoplasm (Fig. 4A,B). The cleaning technique used in the preparation was not able to remove all of the crystals from the replicas. Many crystals were dis-

placed from their corresponding membranes and appeared as clumps of particles (Fig. 4A) in the images, without correspondence to the replica ultrastructure. In some cases, a rim at the periphery of the magnetosomes confirmed the presence of the membrane and indicated that the corresponding crystals were correctly positioned within the magnetosome (Fig. 4B, arrow). It was difficult to observe the membrane in crystal-bearing vesicles due to the high contrast of the magnetosomes. The empty vesicles contained intramembranous particles, similar to those detected in the magnetosome membranes of the magnetite-producing magnetotactic bacterium *Magnetospirillum magnetotacticum* [14]. Unexpectedly, empty P-faces of the vesicles were present in higher numbers than magnetosomes with a crystal inside (56:12), suggesting that the magnetosome membrane of '*Candidatus Magnetoglobus multicellularis*' did not fracture in the same way as common lipid bilayers. Instead, the fracture may have taken place at the crystal-membrane interface, thereby ejecting the crystals from the magnetosomes and exposing the mainly empty P-faces of the vesicles. Mineral-organic interfaces such as those found inside magnetosomes are relatively abundant in nature, but the dynamics of freeze-fracturing at these mineral-membrane interfaces are poorly understood. It is reasonable to assume that the easily fracturing plane lies between

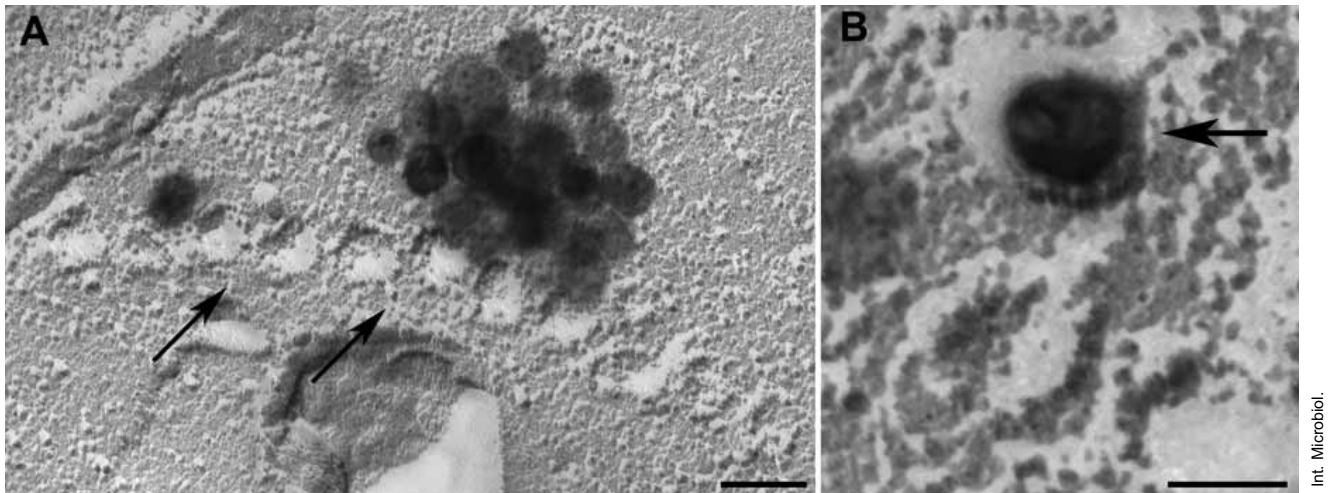


Fig. 4. Freeze-fracture replicas of the cytoplasm of '*Candidatus Magnetoglobus multicellularis*' containing (A) a chain of the P-faces of the magnetosome vesicles, empty vesicles (arrows), and (B) two magnetosome vesicles, one of which contains a crystal (arrow). Scale bar = 100 nm in (A) and 50 nm in (B).

the magnetic crystal and the magnetosome membrane. This, in turn, would indicate that in '*Candidatus Magnetoglobus multicellularis*' either the crystals are poorly attached to the membrane or the membrane differs from the magnetite magnetosome membranes of *M. magnetotacticum* [29].

The observation of a membrane surrounding the magnetosome crystals, their disposition in chains, and their positioning close to the cell surface suggest that a strictly controlled mechanism of biomineralization and crystal orientation operates in '*Candidatus Magnetoglobus multicellularis*.' However, greigite crystals do not have the geometric shapes characteristic of biomineralized magnetite crystals. In addition, the normal size distribution of the greigite crystals in multicellular magnetotactic bacteria contrasts with the log normal size distribution of most magnetite crystals from magnetotactic bacteria [4]. Nonetheless, the greigite magnetosomes are not shapeless, as is true for the iron-oxide minerals produced by *Shewanella putrefaciens* [13], which suggests that '*Candidatus Magnetoglobus multicellularis*' possesses a mechanism that controls crystal morphology. Magnetite and greigite crystal sizes range from 25 to 120 nm [19,31], whereas '*Candidatus Magnetoglobus multicellularis*' produces greigite magnetosomes of up to 180 nm, which are larger than any magnetosome ever described for magnetotactic multicellular prokaryotes. This difference in the sizes of greigite magnetosome crystals could be a function of environmental conditions and/or lower growth rates, or it might reflect the fact that magnetotactic multicellular prokaryotes belong to different species.

The trilaminar membrane unit was not unequivocally observed in all magnetosomes. This may have been related to

the geometry and hardness of the magnetosome crystal. Greigite magnetosomes sizes are compatible with full embedding within a 100-nm electron microscopy ultrathin section (see Table 1; [19]) while iron-sulfide magnetosomes can be cut by diamond knives during ultramicrotomy in such a way that sometimes only parts of the crystals are observed [23]. Thus, the trilaminar structure would only be evidenced when specific faces of the crystal are parallel to the electron microscopy beam. In early studies of *Magnetospirillum magnetotacticum* ultrastructure using conventional TEM preparations, the layer surrounding the magnetosome crystals did not appear as a trilaminar membrane structure; instead, there was a 1.4-nm-thick electron-dense layer surrounding each particle and separated from the crystal surface by an electron-transparent layer of 1.6 nm [5]. These layers are very similar to those observed in '*Candidatus Magnetoglobus multicellularis*' crystals. In this study, a trilaminar membrane unit was observed to surround most of the magnetosomes, as previously described for magnetite magnetosomes [6]; this was especially the case following potassium-ferrocyanide staining.

Based on these results, several conclusions on the nature of the magnetosome membrane in greigite magnetosomes can be drawn. First, the magnetosome membrane appears to stabilize large numbers of magnetosomes, probably by connecting them to the cell surface and/or to a striated structure described recently [34]. Second, the formation of magnetosome chains in '*Candidatus Magnetoglobus multicellularis*' may be similar to the process described in *M. gryphiswaldense*, which depends on magnetic interactions within the chain and on the interactions of proteins [32]. Therefore, the magnetosome membrane would be essential to magnetosome

biomineralization and organization in chains. Both of these processes are fundamental for the generation of a magnetic moment capable of aligning the microorganism along magnetic field lines during movement. Lastly, epigenetic inheritance of the magnetic polarity relative to the axis of movement, as proposed in a recent model for the proliferation of '*Candidatus Magnetoglobus multicellularis*,' would depend on magnetosome anchoring in the cell, which would be a magnetosome-membrane related function [18,19,38].

Acknowledgements. We thank Mr. Raphael Marques for help in the cytochemistry experiments. Financial support from the Brazilian CNPq (Pronex) and FAPERJ is acknowledged.

References

1. Abreu F, Silva KT, Martins JL, Lins U (2006) Cell viability in magnetotactic multicellular prokaryotes. *Int Microbiol* 9:267-272
2. Abreu F, Martins JL, Silveira TS, Keim CN, Lins de Barros HGP, Gueiros-Filho F, Lins U (2007) '*Candidatus Magnetoglobus multicellularis*', a multicellular magnetotactic prokaryote from a hypersaline environment. *Int J System Evol Microbiol* 57:1318-1322
3. Angermüller S, Fahimi HD (1982) Imidazole-buffered osmium tetroxide: an excellent stain for visualization of lipids in transmission electron microscopy. *Histochem J* 14:823-835
4. Arató B, Szányi Z, Flies C, Schüler D, Frankel RB, Buseck PR, Pósfai M (2005) Crystal-size and shape distributions of magnetite from uncultured magnetotactic bacteria as a potential biomarker. *Am Mineral* 90:1233-1241
5. Balkwill DL, Maratea D, Blakemore RP (1980) Ultrastructure of a magnetotactic spirillum. *J Bacteriol* 141:1399-1408
6. Bäuerlein E (2003) Biomineralization of unicellular organisms: an unusual membrane biochemistry for the production of inorganic nano- and microstructures. *Angew Chem Int Ed* 42:614-664
7. Bazylinski DA (1999) Synthesis of the bacterial magnetosome: the making of a magnetic personality. *Int Microbiol* 2:71-80
8. Bazylinski DA, Frankel RB, Heywood BR, Mann S, King JW, Donaghay PL, Hanson AK (1995) Controlled biomineralization of magnetite (Fe₃O₄) and greigite (Fe₃S₄) in a magnetotactic bacterium. *Appl Environ Microbiol* 61:3232-3239
9. Bazylinski DA, Garratt-Reed AJ, Frankel RB (1994) Electron microscopic studies of magnetosomes in magnetotactic bacteria. *Microsc Res Tech* 25:389-401
10. Devouard B, Pósfai M, Hua X, Bazylinski DA, Frankel RB, Buseck PR (1998) Magnetite from magnetotactic bacteria: size distribution and twinning. *Am Mineral* 83:1387-1398
11. Farina M, Esquivel DMS, Lins de Barros HGP (1990) Magnetic iron-sulphur crystals from a magnetotactic microorganism. *Nature* 343:256-258
12. Frankel RB, Dunin-Borkowski RE, Pósfai M, Bazylinski DA (2007) Magnetic microstructure of magnetotactic bacteria. In: Bäuerlein E, Behrens P, Epple M (eds) *Handbook of biomineralization*. Wiley-VCH Weinheim, Germany, pp 127-144
13. Glasauer S, Langley S, Beveridge TJ (2002) Intracellular iron minerals in a dissimilatory iron-reducing bacterium. *Science* 295:117-119
14. Gorby YA, Beveridge TJ, Blakemore RP (1988) Characterization of the bacterial magnetosome membrane. *J Bacteriol* 170:834-841
15. Hanzlik M, Winklhofer M, Petersen N (2002) Pulsed-field-remnance measurements on individual magnetotactic bacteria. *J Magn Magn Mat* 248:258-267
16. Hayat MA (2000) *Principles and techniques of electron microscopy: biological applications*. 4th edn, Cambridge Univ. Press, Cambridge, 626 pp
17. Keim CN, Abreu F, Lins U, Lins de Barros HGP, Farina M (2004) Cell organization and ultrastructure of a magnetotactic multicellular organism. *J Struct Biol* 145:254-262
18. Keim CN, Martins JL, Abreu F, et al. (2004) Multicellular life cycle of magnetotactic prokaryotes. *FEMS Microbiol Lett* 240:203-208
19. Keim CN, Martins JL, Lins de Barros HGP, Lins U, Farina M (2007) Structure, behavior, ecology and diversity of multicellular magnetotactic prokaryotes. In: Schüler D (ed) *Magnetoreception and magnetosomes in Bacteria*. Springer, Heidelberg, Germany, pp 103-132
20. Keim CN, Solórzano G, Farina M, Lins U (2005) Intracellular inclusions of uncultured magnetotactic bacteria. *Int Microbiol* 8:111-117
21. Komeili A, Vali H, Beveridge TJ, Newman DK (2004) Magnetosome vesicles are present before magnetite formation, and MamA is required for their activation. *Proc Nat Acad Sci USA* 101:3839-3844
22. Komeili A, Li Z, Newman DK, Jensen GJ (2006) Magnetosomes are cell membrane invaginations organized by the actin-like protein MamK. *Science* 311:242-245
23. Lins de Barros HGP, Esquivel DMS, Farina M (1990) Biomineralization of a new material by a magnetotactic microorganism. In: Frankel RB, Blakemore RP (eds) *Iron biominerals*. Plenum Press, New York, pp 257-268
24. Lins U, Farina M (2001) Amorphous mineral phases in magnetotactic multicellular aggregates. *Arch Microbiol* 176:323-328
25. Lins U, Freitas F, Keim CN, Lins de Barros H, Esquivel DMS, Farina M (2003) Simple homemade apparatus for harvesting uncultured magnetotactic microorganisms. *Braz J Microbiol* 34:111-116
26. Lins U, Freitas F, Keim CN, Farina M (2000) Electron spectroscopic imaging of magnetotactic bacteria: magnetosome morphology and diversity. *Microsc Microanal* 6:463-470
27. Lins U, Keim CN, Evans FF, Farina M, Buseck PR (2007) Magnetite (Fe₃O₄) and greigite (Fe₃S₄) crystals in multicellular magnetotactic prokaryotes. *Geomicrobiol J* 24:43-50
28. Mann S, Sparks NHC, Blakemore RP (1987) Structure, morphology and crystal growth of anisotropic magnetite crystals in magnetotactic bacteria. *Proc R Soc Lond Ser B* 231:477-487
29. Martins JL, Keim CN, Farina M, Kachar B, Lins U (2007) Deep-etching electron microscopy of cells of *Magnetospirillum magnetotacticum*: evidence for filamentous structures connecting the magnetosome chain to the cell surface. *Curr Microbiol* 54:1-4
30. Pósfai M, Buseck PR, Bazylinski DA, Frankel RB (1998) Iron sulfides from magnetotactic bacteria: structure, composition, and phase transitions. *Am Mineral* 83:1469-1481
31. Pósfai M, Cziner K, Márton P, Buseck PR, Frankel RB, Bazylinski DA (2001) Crystal-size distributions and possible biogenic origin of Fe sulfides. *Eur J Mineral* 13: 691-703
32. Scheffel A, Gruska M, Faiure D, Linaroudis A, Plitzko JM, Schüler D (2006) An acidic protein aligns magnetosomes along a filamentous structure in magnetotactic bacteria. *Nature* 440:110-114
33. Schüler D (2007) *Magnetoreception and magnetosomes in bacteria*. Microbiological monographs 3. Springer, Heidelberg, Germany, 319 pp
34. Silva KT, Abreu F, Almeida FP, Keim CN, Farina M, Lins U (2007) Flagellar apparatus of south-seeking many-celled magnetotactic prokaryotes. *Microsc Res Tech* 70:10-17
35. Simmons SL, Edwards KJ (2007) Unexpected diversity in populations of the many-celled magnetotactic prokaryote. *Environ Microbiol* 9:206-215
36. Taylor AP, Barry JC (2004) Magnetosomal matrix: ultrafine structure may template biomineralization of magnetosomes. *J Microsc* 213:180-197
37. Thornhill RH, Burgess JG, Sakaguchi T, Matsunaga T (1994) A morphological classification of bacteria containing bullet-shaped magnetic particles. *FEMS Microbiol Lett* 115:169-176
38. Winklhofer M, Abraçado LG, Davila AF, Keim CN, Lins de Barros HGP (2007) Magnetic optimization in a multicellular magnetotactic organism. *Biophys J* 92:661-670